Scientific Research Publishing

Open Journal of Geology, 2025, 15(2), 69-86
https://www.scirp.org/journal/ojg
ISSN Online: 2161-7589
ISSN Print: 2161-7570

South American Breakup and Andean Torque Deformation

Adolfo Antonio Gutiérrez

Faculty of Natural Sciences and Miguel Lillo Institute, National University of Tucumán, Tucumán, Argentina
Email: gutierrez.aa@hotmail.com

How to cite this paper: Gutiérrez, A.A. (2025) South American Breakup and Andean Torque Deformation. *Open Journal of Geology*, **15**, 69-86.
https://doi.org/10.4236/ojg.2025.152003

Received: November 28, 2024
Accepted: February 17, 2025
Published: February 20, 2025

Abstract

Geological deformations are generally attributed to compressional, extensional and strike-slip processes. Since the breakup of Gondwana, torque deformation has been responsible for the current configuration of the western coasts of Africa and the eastern shore of South America and the morphotectonic geometry of the rift basins of South America, conditioning the morphostructure of the Andean chain and the current geoforms of the foreland.

Keywords

Tectonic, Torque Deformation, Continental Drift, Rift Valley, South America

1. Introduction

Towards the end of the Proterozoic, Africa and South America were joined together as part of the Gondwana continent, composed of Archean and Mesoproterozoic cores, bordered by Neoproterozoic orogenic belts [1] (**Figure 1**). We can follow the trajectory and position of South America relative to Africa after the breakup of Gondwana through the arrangement of the magnetic bands on the ocean floor generated by the hot spots [1] (**Figure 1**). Since the first ideas of similar landforms between the coasts of South America and Africa and the formation and or destruction of continents postulated by Wegener [2] [3], numerous works have followed, arguing that these continents were joined towards the end of the Jurassic and separated by extension [4]-[8]. All of them show a scheme where the current morphostructure of the eastern edge of South America, with some modifications, was geometrically assembled with the western edge of Africa (**Figure 1**). Focal mechanism solutions for earthquakes occurring near fracture zones that offset the Mid-Atlantic Ridge are consistent with normal faults along N-S planes and, right-handed transform

faults displaced these segments [3].

Figure 1. Cartographic scheme that places Africa and South America together at the beginning of the breakup of Gondwana. The map shows the main geological units of both continents as well as the trajectories of the magnetic bands generated by the hot spots (Based on [1]-[3] [9] [10]). SE: Santa Elena hot spot and its trajectory. W: Walvis hot spot and its trajectory.

The structural geometry of Triassic, Jurassic and Cretaceous rift basins appears to follow the Mid-Atlantic Ridge rift model.

Based on morpho-structural patterns considered as kinematic mega-indicators obtained from the interpretation of satellite images, bibliographic information and structural data obtained in the Eastern Cordillera, Santa Barbara System, and Sierras Pampeanas, a torque deformation scheme is proposed for South America. Since the breakup of Gondwana, this deformation system has been responsible for the current configuration of the western coasts of Africa and the eastern shore of South America and the morphotectonic geometry of the rift basins of South America, conditioning the morphostructure of the Andean chain and the current geoforms of the foreland.

2. Study Area

The study area covers the entire South American continent, considering South America still attached to Africa (**Figure 1**). The separation of both continents, the

Triassic, Jurassic and Cretaceous rift basins generated during the South American drift, and the regional structures and geometries generated as a consequence of the South American drift and the collision with the ridges and the Nazca Plate are analyzed.

3. Methodology

The work methodology consisted of reading and interpreting radar images (from the SRTM Radar) and LANDSAT, ASTER and Sentinel satellite images. The interpretation of these images provided us with an overview and allowed us to analyse large-scale geoforms generated by tectonics. It also helped us to prepare thematic cartography. Field work was carried out in the Santa Barbara System, Eastern Cordillera and Sierras Pampeanas of Argentina. The collection of structural data (normal, reverse, and strike-slip faults, compressional and extensional wedges) and the analysis of the tectonic morphology of these regions (E-W and N-S compression, folded folds in the foreland of the central Argentine Andes, rotation of mountain ranges on a vertical axis, intermontane basins, surface drainage structure) allowed us to carry a regional tectonic deformation model to a larger, continental scale. We observed that these regional morphotectonic models have a geometry and a pattern that is repeated at a macro scale with a common origin. All the field information and that obtained with remote sensing images was complemented with data obtained from the literature (origin of rift basins, radiometric dating, terrestrial rotations on the vertical axis, continental drift, convergence of ridges and plates, etc.). To analyze continental drift, literature and information on the location of hot spots were taken into account. With this base, a reverse path of the drift of the eastern continental margin of South America was carried out until it coincided with Africa. This methodology allowed us to determine and associate the rupture and separation of South America from Africa and the origin of the rift basins with torque deformation. We also determined the approximate location of the pivot points where the levers occurred, the distances traveled with the drift, and the angles of rotation.

4. Research Results

4.1. Torque Deformation

Torque is the rotation of an object around an axis caused by the product of a force and the perpendicular distance from the rotation axis to the force's application point [11] (**Figure 2**). Torque is a magnitude that describes the dynamics of a rotating rigid body, the forces that mobilize objects and systems [11]. When the force acts perpendicularly at a greater distance from the lever arm, the effectiveness of the torque is maximum [11] (**Figure 2(a)**; **Figure 2(b)**. Lower torque is produced depending on the magnitude of the force, the distance of application of the force to the centre of rotation or the direction of application of the force [11] (**Figure 2(c)**). Torque deformation results in secondary forces, rotations, folds, and fractures [12] (**Figure 2(c)**). At the torque support point, there is extension

in the convex area and compression in the concave area [12]-[14] (**Figure 2(c)**). If the force acts on the lever arm at an angle less than 90˚, transpression or transtension generates parallel forces inside the lever arm body that cause shear deformation [12] [15] [16] (**Figure 2(c)**). As the deformation of the fold progresses, extension fractures originate that converge at the support point [12] (**Figure 2**). **Figure 3** illustrates the natural breaking of a tree by torque. The torque on the tree trunk occurred instantaneously, under ambient temperature conditions. In detail, the torque generates fractures and deformation geometries similar to those found in rocks (**Figure 3(b)**). On the scale of South America, the torque occurred over a period of about 148 Ma, on rocks with different rheological properties, taking advantage of pre-existing fractures and with heat sources provided by the magmatic rise. There is a clear and large difference in the geometries of the structures and in the tectonic morphology of the regions deformed by compression, extension and torque. In the Sierras Pampeanas of Argentina there are examples of torque deformation related to NE-oriented compressive forces [13] [14] [17] [18].

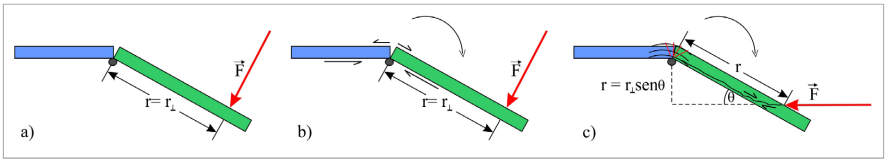

Figure 2. a) The figure illustrates the rotation of a door on its hinges. Torque has both magnitude and direction. By definition, torque is the physical vector quantity that causes the object to rotate, and it is the vector product of the distance from the pivot to the force with the force: $\tau = F \cdot r$ [11]. b) A torque produced by a force perpendicular to the lever, acting at a distance r from the fulcrum, is illustrated. Converging and diverging forces acting at the fulcrum are also indicated. c) A lower torque is produced if the force of the same magnitude as in a) acts at the same distance as a) but with an angle less than 90˚. In this case, the rotation does not occur in a hinge-like, with the lever freely rotating at the fulcrum. Both bodies are connected, and due to the torque, folds (curved black lines) and stress fractures (straight red lines, which converge to the concave area of the fulcrum) are produced on the external side of the fulcrum. The transpressive or transtensive force of the torque generates a horizontal displacement in the lever arm.

4.2. South American Drift

According to the literature, the separation of South America and Africa occurred through extension, giving rise to the Atlantic Ocean. This extension is supposed to cause horizontal displacement and rotation in South America, generating continental drift. Three domains exist along the margins of South America and Africa [19]. The South Atlantic extensional domain developed from the southern tip of Argentina to the northeastern tip of Brazil. The location of the magnetic poles is evidence that during the Late Triassic to the Sinemurian, the South American continent would have been located in its southernmost position, then moved northwards, where it remained until the end of the Early Jurassic (**Figure 4**). Finally, South America moved southwards again, and in the Middle Jurassic, it reached latitudes of almost 30˚S similar to those present [20] (**Figure 4**). In the

Equatorial Atlantic domain, a dextral strike-slip trend developed with an E-W direction and produced the rupture of the crust, creating a pattern of high-angle oblique faults that controlled rifting and resulted in the development of large-scale fracture zones parallel to the coast between the Aptian and the Cenomanian (Figure 4). The third Central Atlantic extensional domain is in the region north of the mouth of the Amazon River, whose first rifting phase occurred in the Triassic.

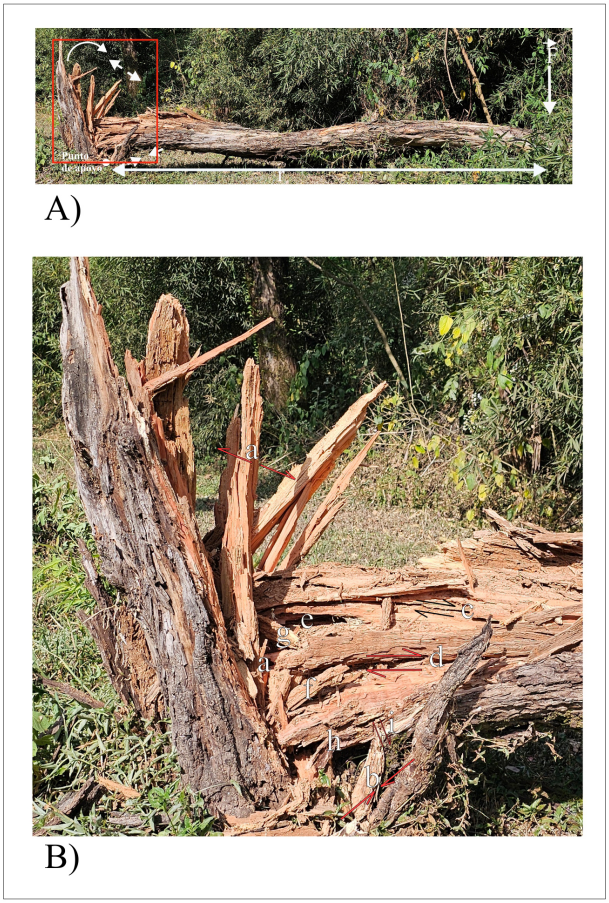

Figure 3. Illustration of natural torque produced on a tree. A) In the photo, observe the pivot or support point, the location of the force exerted and the distance "r" between the pivot and the force. The direction of rotation due to the strain exerted and the areas where extension and compression occur are with white arrows. The red box is the location in B. B) Detail the geometry of the fractures generated by the torque. Letters and arrows indicate a) Extension zone. b) Compression zone. c) and d) Zones of dextral horizontal displacement. e) Gaps. f) and g) Tree branches arranged in different orientations. h) Folds. i) Reverse displacement.

Euler's theorem describes the relative motion between two plates on the Earth's surface by angular separation around a pole of relative motion, known as the Euler Pole [3]. Thus, in relative plate motion, the pole of any two plates tends to remain fixed relative to each other for long periods, even though the plate velocities are equally constant over periods of several million years [3].

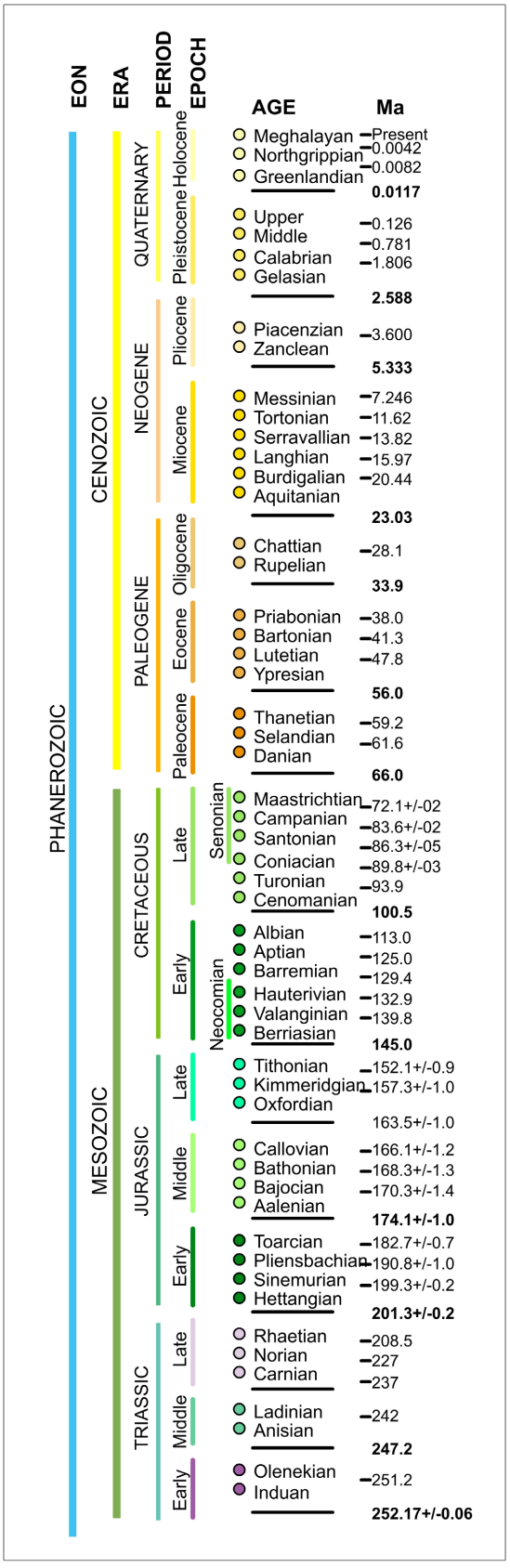

Figure 4. Geological ages. Modified from the international commission on stratigraphy [26].

4.3. Deformation during the Triassic-Jurassic

Western South America was situated on an eastward-tilted subduction zone since the Paleozoic and contraction events shortened the crust in the back arc during the Carboniferous, Permian and Jurassic [7] (**Figure 4**). The opening of the Atlantic Ocean between South America and Africa begins with convection currents in the Earth's mantle that generate the forces that push the plates [1] [21]. The opening of the Atlantic extended from the Upper Jurassic in the south (Rawson-Outeniqua segment) to the north (Pelotas/Walvis segment) in the Barremian [4] [22] [23] (**Figure 4**). Between 138 and 127 Ma (Ar^{40}/Ar^{39} geochronology) [24], effusive activity at the Walvis hotspot gave rise to the Serra Geral Basalts in the Paraná and Etendeka Basin in Namibia [1] (**Figures 4-6**). The breakup of Gondwana generated semi-grabens on the continent due to the reactivation of Paleozoic structures [4] that were filled with continental volcaniclastic deposits from the Late Triassic to the Early Jurassic, related to dextral displacement along the main strike-slip faults that limit the continental plates [4] [25].

These basins were associated with N, NW-trending horizontal faults and dextral displacement, such as the Gastre fault system, and some blocks underwent rotation [4] [20] [23] [25]. The clockwise rotations observed in the rocks of the Deseado Massif, which occurred between the Jurassic and the Early Cretaceous, document the deformation of southern Patagonia during the breakup of western Gondwana [27] (**Figure 4**).

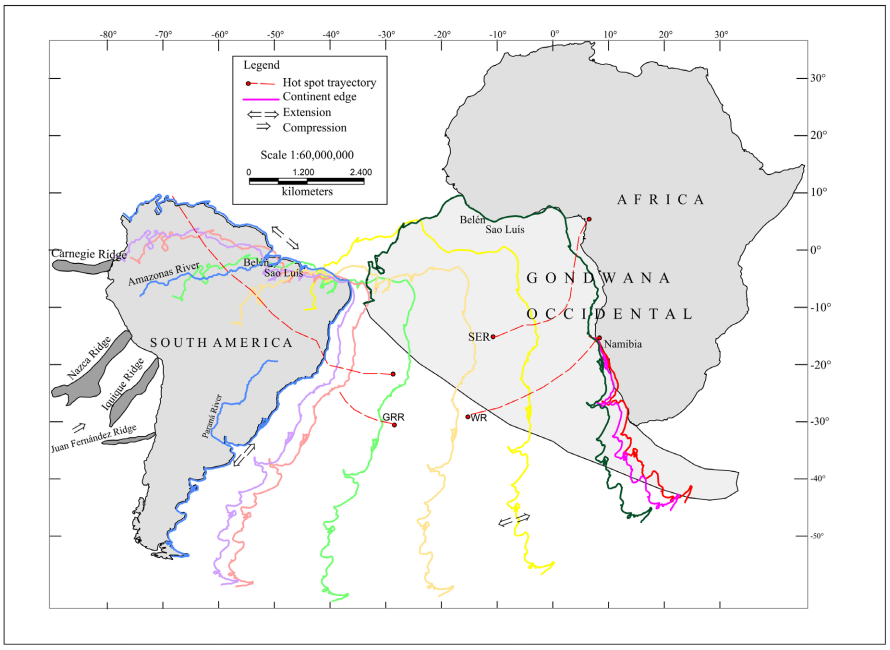

Figure 5. The map shows the assembly between South America and Africa towards the end of the Triassic before the breakup of Gondwana. The coloured lines represent the edge of South America, indicating a displacement that follows a hypothetical path to its current position. SER: Santa Elena Ridge hot spot and its trajectory. WR: Walvis Ridge hot spot and its trajectory. The map also indicates the approximate distances that mark the path of the South American drift and the approximate clockwise rotations (Drawn based on [22] [28]).

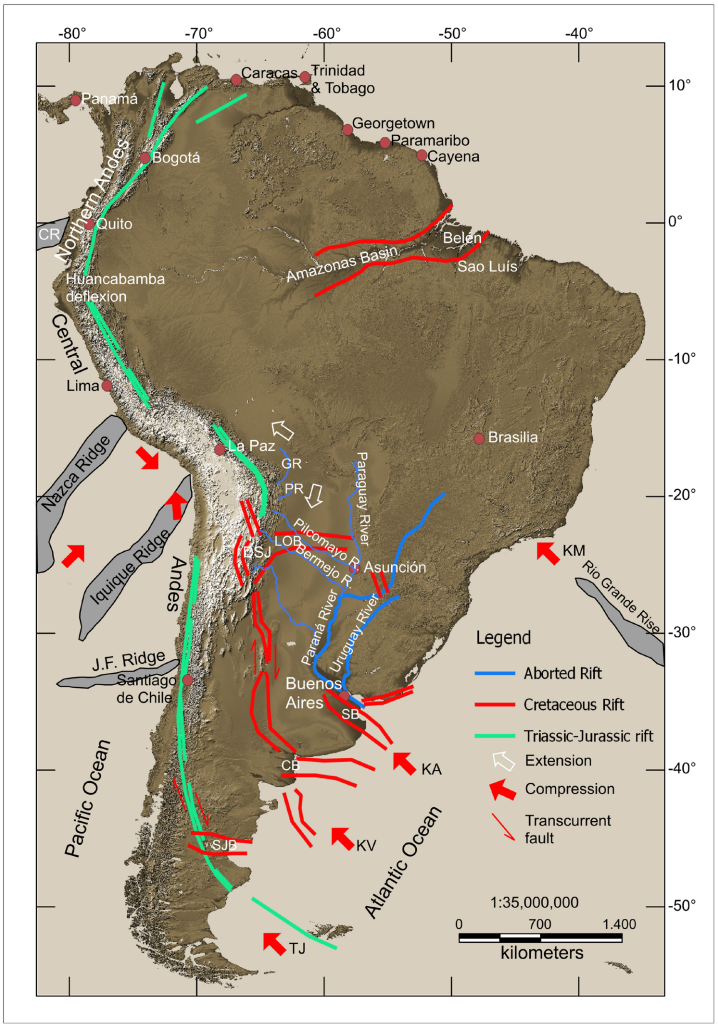

Figure 6. Image map of South America showing a morphotectonic scheme. TJ (Triassic-Jurassic), KV (Cretaceous, Valanginiano), KA (Cretaceous, Albiano), KM (Cretaceous, Mastrichtiano): Positions in time of the principal strain. GR: Grande River. CR: Carnegie Ridge. PR: Parapetí River. DSJ: Dorsal Salto-Jujeña. CB: Colorado Basin. SJB: San Jorge Basin. SB: Salado Basin. LOB: Lomas de Olmedo Basin. Drawn from [4] [21] [23] [29].

4.4. Deformations in the Mesozoic

The opening of the South Atlantic Ocean in the Early Cretaceous cut Paleozoic-Mesozoic cratons and sedimentary basins and caused the South American plate to push westward at a speed of 3 cm/year, separating Africa from South America, controlling variations in the convergence rate along the subduction zone [1] [2] [21] [30]. South America increased westward drift after the Cenomanian [31] (**Figure 4**).

The Cretaceous basins of the Sierras de Córdoba originated by dextral strike-slip faults, arranged in an echelon, associated with the Eastern Pampean Lineament that presents a dextral horizontal displacement [29]. The largest depocenter of the Cretaceous rift is formed in northern Argentina by the Tres Cruces and Metan-Alemanía basins, which trend NNW, and the Lomas de Olmedo basin, which

trend east-west. The latter represents the basin's most active and deepest depocenter, limited to the north by the Michicola Ridge, whose faults reach more than 6 km of rejection, and to the south by the Quirquincho Arch [32]. Radiometric dating of the eruptive rocks in the Pirgua Subgroup sequence indicates ages of 128.95 Ma and 78.75 Ma [33] (**Figure 4**). In South America, the Triassic basins were reactivated during the Cretaceous, spreading in an NNW strike from the Salado and Colorado basins, covering a large part of NW Argentina to southern Bolivia [1]. The Amazon and Marajó basins were formed during the extensional tectonic phase of the middle Cretaceous to early Tertiary [34], and the Amazon River began as a transcontinental river between 11.8 and 11.3 Ma [35] (**Figure 4**). The definitive opening of the Atlantic Ocean in the equatorial zone during the Albian was the beginning of the absolute displacement of the South American plate, starting the compressive deformation in the segments of Peru and Colombia at 100 Ma [30] (**Figure 4**).

4.5. Deformations in the Cenozoic

The geometry of the Nazca Plate beneath the South American continental plate [36] [37] is related to the collision zones between the Nazca and Juan Fernández ridges with the edge of the continent [38]-[40]. The first widespread contractive events in the Andean Cycle appear to have occurred in Santonian-Campanian times, shortly after the final disconnection between Africa and South America in the present-day Equatorial Atlantic [41] (**Figure 4**). A Cretaceous-Paleogene (pre-Andean) episode of back-arc bending subsidence is recognized, followed by a Neogene Andean episode of crustal shortening reflecting the eastward propagation of the orogenic wedge to its present position ([7]. Between 14˚ - 28˚ S, the volcanism that occurred from 65 to 0 Ma is closely related to deformation, in particular, the preferential grouping of volcanic centres at the intersections of the frontal arc with areas of NW-trending lineaments [42]. In the Luracatao and Calchaquí valleys, there is evidence of these Paleogene deformations [43] (**Figure 4**). Some morpho-tectonic processes in the Andes, such as horizontal rotations and N-S compressions, cannot be fully explained by plate kinematics or simple compression-extension schemes [44]-[51]. In the Chilean forearc, strike-slip faults parallel to the margin develop, which do not seem to depend on the velocity or obliquity of convergence or the mode of mass transfer at the subduction front [52]. Different sectors of the Andes show a great variety of complex processes, such as mountain formation, which do not fit the type of non-collisional orogen that formed a mountain chain by subduction of oceanic crust under a continental plate, proposed by other authors [21]. On the Atlantic coast of Tierra del Fuego, the front of the Fuegian Andes fold and thrust belt migrated northwards due to compression 50 - 40 Ma ago, which may have ceased in the Early Miocene [53] (**Figure 4**). The folded folds involving Neogene strata in the foreland of the Central Andes of the Precordillera, Sierras Pampeanas, Famatina System, Eastern Cordillera and Santa Bárbara System show an NNE shortening [51]. Different models explain the pattern of rotations observed in the Andean margin [44] [45] [54]-[57]. Paleomagnetic analyses of Jurassic to

Neogene rocks in the flat subduction Pampean segment and the south, in the high-angle subduction segment, show clockwise rotations of up to 40˚ induced by a coupled model of the Bolivian Orocline-Juan Fernández Ridge [58]. In the Neogene, Andean tectonics caused crustal shortening, shaping the morphology of the South American foreland [59] [60]. Clockwise tectonic rotations are one of the most important structural features of the Andes of northern Chile, generated by transpressional deformation that affected large areas during the deformation that occurred in the Eocene and lower Oligocene [61] [62] (**Figure 4**). The zone with the most remarkable shortening of the Andes is central Bolivia [63]. The hypotheses on the formation of oroclines refer to forces acting perpendicular to the axis of the orogen [64] or parallel to the axis of the orogen [65] generating a triangular tension zone in the convex part of the oroclines [44]. Paleomagnetic data of Paleozoic rocks show counterclockwise rotations in southern Peru and clockwise rotations in northern Chile and indicate that the Bolivian Orocline was formed during the Eocene-Oligocene by differential horizontal shortening coinciding with the most significant shortening of the Eastern Cordillera in this period [49] [66] (**Figure 4**). Paleomagnetic results document a pattern of clockwise (25˚ + 11.6˚) rotations after the Paleocene and counterclockwise (19˚ + 9.7˚) rotations after the early Oligocene north and south, respectively, of the Huancabamba bypass, the coastal area of northern Peru (04˚ LS) [67] (**Figure 4**). These results are consistent with those obtained from Cretaceous formations [68] and with those obtained from Mesozoic formations [69], which indicate counterclockwise rotations of −30˚ south of the Huancabamba bypass. The WNW and NW shortening that reflects the Miocene and Pliocene structures, respectively, in the Uyuni-Atacama region, seems to be related to a rearrangement due to the absolute movement of the South American Plate to the WNW [70] (**Figure 4**). The Andes' escape towards the NE occurred during the 1.8 Ma due to the subduction of the Carnegie Ridge beneath the South American plate [71], and the Santa Marta Massif experienced a clockwise rotation on the vertical axis in the Upper Eocene [72] (**Figure 4**).

5. Discussion and Results

5.1. South America Trayectory

Convection currents in the Earth's mantle generated the forces that exerted pressure on southern Argentina, and the South American plate began a process of torque deformation. In our concept of the deformation of South America, the horizontal and rotational movements of the continental plate were not independent of each other; they did not act separately. The rotation did not occur as a hinge (**Figure 2(a)**), turning the entire continental plate of South America as if it were a solid monolithic block. On the contrary, these movements acted together at some point. The rupture and horizontal displacement of the Mid-Atlantic Ridge at a point in the south began to move the continental block that was anchored at its northern end (cratonic zones), generating an internal deformation by Torque (**Figure 2(c)** and **Figure 3**). The ruptures occurred in those areas of greatest weakness, intra-

cratonic, keeping the cratonic zones together. We started a reverse path of the trajectory of South America, from its current position to its joining with the edge of Africa (**Figure 5**), trying to follow the arrangement of the magnetic bands of the ocean floor generated by the hot spots [1] [22] [28] (**Figure 5**). The geometric argument of the joining edges between South America and Africa is coherent, considering that between them there was a rupture and detachment by an extensive, constructive process. The western edge of South America must have been different from the current morphostructure because, since the separation of the continents in the Cretaceous, it has suffered destruction by compressive tectonic processes (**Figure 5**). The first movement shows the southern coast of South America, which is slightly away from the southern coast of Africa, and the continents remain joined in the north (**Figure 5**; indicated by the red line). This union marks the deformation's beginning with torque and clockwise rotation. In the second stage, South America begins to detach from Africa, the rotation continues, and the torque's support point is in Namibia (**Figure 5**; position of the pink line). The deformation continues with clockwise rotation, and the torque now has its support point in the current areas of Belén and Sao Luís (**Figure 5**; position of the dark green line). From the initial position of South America joined with Africa to the position of the light green line, the eastern edge of South America suffered a clockwise rotation and began to drift towards the SW (**Figure 5**). Finally, South America moves west and north to its current position (blue line) from the position occupied by the eastern edge with the light green line (**Figure 5**). This journey undergoes a clockwise rotation also (**Figure 5**).

5.2. Morphotectonic Processes in South America

Towards the Triassic-Jurassic, the force generated by convection in the Earth's mantle was in the extreme south of Argentina (**Figure 4**); the pivot zone was located about 1800 km and 3100 km to the north, at the southern end of Africa (**Figure 5**; red and pink lines) and (**Figure 6**). The South American plate began a clockwise rotation path (**Figure 5**). This torque deformation maximized the effectiveness of rifting and basin formation on the continental sector, where the geological units offered less resistance (**Figure 1** and **Figure 6**). The zones occupied by cratonic rocks (West Africa, Amazonia, Sao Francisco, Congo, Rio de la Plata, Kalahari) (**Figure 1**) served as support and pivot points for the torque. The force exerted transtension on the southern edge of the rift basins (**Figure 6**). This geometry allowed the formation of the Triassic and Jurassic rift basins along the western edge of South America, the dextral displacement of the faults that limit it and the clockwise rotation of some blocks (**Figure 6**). This torque deformation process caused a clockwise rotation of South America from its initial position to the location of the eastern edge indicated by the dark green line (**Figure 5**).

The forces that dominated the displacement of South America in the Early Cretaceous were in the region of the Colorado and Salado basins (**Figure 6**), whose lever arms were about 4400 km away from the pivot point in the Belén-Sao Luis area (**Figure 5** and **Figure 6**). These forces opened the Cretaceous rift basins in

the continental zones, bordering the Amazon, Río Apa and Río de la Plata cratonic zones to the west (**Figure 1** and **Figure 6**). The Paraná River basin in Argentina did not develop fully and constituted an aborted rift (**Figure 6**). The edge of South America, represented by the dark green line (**Figure 5**), had already begun to separate but was still very close to the coast of Africa. The displacement of South America continued to the SW, to the position occupied by the light green line (**Figure 5**). The Amazon basin has an NE orientation similar to the Olmedo Basin in Argentina (**Figure 6**). Both were formed in the Cretaceous and are oriented perpendicular to the remaining Triassic, Jurassic and Cretaceous basins (**Figure 6**). The Amazon and Olmedo basins are likely to have been formed by extension generated by the torque in the outer part of the system, when the continents finally separated, as shown in **Figure 2(c)** and **Figure 3**. At that time the torque acquired greater magnitude until it finally broke the cratonic zones of Amazonia and west Africa (**Figure 1**).

South America begins a journey towards the west and north from the light green line, continuing with the clockwise rotation (**Figure 5**). This geometry means that the convergence is not strictly compressive, as reported in the literature. The Rio Grande Ridge (RGR) and the Walvis Ridge (WR) (**Figure 5** and **Figure 6**) are large igneous provinces in the South Atlantic, formed on the South American and African plates, respectively, mainly by the volcanism of a hot spot that erupted between 83.6 Ma and 66.4 Ma [73] (**Figure 4**). At this time, we locate the east coast of South America at the position of the light green line (**Figure 5**). The Rio Grande Ridge exerts the strength that moves South America in an NW direction (**Figure 6**). Its position in the central area of South America displaces it towards the NW, where the ridges collide with the west coast of the continent at different angles of incidence (**Figure 5** and **Figure 6**). The violet line marks the position of South America when it probably begins to interact with the Juan Fernández Ridge in the Upper Eocene, as indicated by different authors in the literature [50] (**Figure 4** and **Figure 5**). Later, Iquique, Nazca and Carnegie ridges collide with the west shore of the South American Plate (**Figure 5**). To reach its current position (blue line), South America must still travel to north with a clockwise rotation (**Figure 5**). A new stage of torque deformation begins on the west coast of South America, which gave rise to the Andean chain (**Figure 6**). The joint action of the Río Grande, Juan Fernández and Nazca ridges generated The Bolivian Orocline by transpression and torque. Each ridge collision with the west coast of South America constitutes a support and pivot point, developing a rotation with horizontal and vertical displacement. The speed of movement of the Juan Fernández Ridge was greater than that of the South American plate [2] [30] [39]. The Nazca Plate pushed towards the NE and the South American Plate towards the NW, resulting in an north trajectory (**Figure 6**).

6. Conclusions

The separation of South America from Africa was produced by torque and induced by convection currents in the Earth's mantle, which generated the forces that

pushed the plates (Figure 5 and Figure 6). The Triassic, Jurassic and Cretaceous basins were formed by a torque deformation process, as were other Andean structures such as block rotations and the Bolivian Orocline (Figure 2(c) and Figure 3). In the foreland of the Bolivian Orocline, the divergence of surface runoff from the drainage in the Central Andes occurs towards the NE and the SE, evidenced by the Grande, Parapetí and Pilcomayo, Bermejo rivers, respectively (Figure 6). The extension generated by the torque formed the ENE-trending Cretaceous basins of Amazonas and Lomas de Olmedo (Figure 2(c) and Figure 3). The geometry of the Lomas de Olmedo basin likely gave rise to the Mesopotamia of Formosa, limited by the Pilcomayo and Bermejo rivers (Figure 6). A similar process would have given rise to the Mesopotamia of the Litoral, limited by the Paraná and Uruguay rivers (Figure 6).

The westward displacement of South America (Figure 5: from the light green line) generated the first contractive events of the Andean cycle in the Upper Cretaceous (Santonian-Campanian) (Figure 4). Since the Upper Eocene, the deformation process on the west coast of the South American Plate has been controlled by the NE convergence of the ridges and by the northwest trajectory of South America (Figure 4 and Figure 5). These collisions will cause South America to have a final clockwise rotation and a northward drift (Figure 5). This deformation process explains the north-south contraction that occurs in the Central Andes. The NE and NW strikes of the Andean chain and the opposite rotations on both sides of the Huancabamba deflection coincide with the geometry of the Amazon basin (Figure 6). These geometries suggest that they were produced by the joint action of the Carnegie and Rio Grande ridges, taking advantage of the structural weakness of the Amazon basin (Figure 6).

Acknowledgements

The National University of Tucumán and the Argentine-German University Center contributed to support our research. Special thanks to the reviewers who contributed to improving the manuscript with their corrections and suggestions.

Conflicts of Interest

The author declares no conflicts of interest regarding the publication of this paper.

References

[1] Benedetto, J.L. (2018) El continente de Gondwana a través del tiempo. Una introducción a la Geología Histórica. Academia Nacional de Ciencias.

[2] de Wit, M.J., de Brito Neves, B.B., Trouw, R.A.J. and Pankhurst, R.J. (2008) Precenozoic Correlations across the South Atlantic Region: (The Ties That Bind). *Geological Society*, *London*, *Special Publications*, **294**, 1-8. https://doi.org/10.1144/sp294.1.

[3] Kearey, P., Klepeis, K.A. and Vine, F.J. (2009) Global Tectonics. 3rd Edition, Wiley-Blackwell.

[4] Uliana, M.A., Biddle, K.T. and Cerdan, J. (1989) Mesozoic Extension and the Formation

of Argentine Sedimentary Basins. In: *Extensional Tectonics and Stratigraphy of the North Atlantic Margins*, American Association of Petroleum Geologists, 599-614. https://doi.org/10.1306/m46497c39

[5] Salfity, J.A. and Marquillas, R.A. (1994) Tectonic and Sedimentary Evolution of the Cretaceous-Eocene Salta Group Basin, Argentina. In: *Cretaceous Tectonics of the Andes*, Springer Vieweg Verlag, 266-315. https://doi.org/10.1007/978-3-322-85472-8_6

[6] Mon, R. and Salfity, J.A. (1995) Tectonic Evolution of the Andes of Northern Argentina. In: Tankard, A.J., Suárez Soruco, R. and Welsink, H.J., Eds., *Petroleum Basins of South America*, American Association of Petroleum Geologists Memoir, 269-283.

[7] McGroder, M.F., Lease, R.O. and Pearson, D.M. (2015) Along-Strike Variation in Structural Styles and Hydrocarbon Occurrences, Subandean Fold-and-Thrust Belt and Inner Foreland, Colombia to Argentina. In: DeCelles, P.G., Ducea, M.N., Carrapa, B. and Kapp, P.A., Eds., *Geodynamics of a Cordilleran Orogenic System*: *The Central Andes of Argentina and Northern Chile*, Geological Society of America. https://doi.org/10.1130/2015.1212(05)

[8] Romano, M. and Cifelli, R.L. (2015) 100 Years of Continental Drift. *Science*, **350**, 915-916. https://doi.org/10.1126/science.aad6230

[9] Vaughan, A.P.M. and Pankhurst, R.J. (2008) Tectonic Overview of the West Gondwana Margin. *Gondwana Research*, **13**, 150-162. https://doi.org/10.1016/j.gr.2007.07.004

[10] https://www.es.wikipedia.org/wiki/cratón_amazónico

[11] Ling, S.J., Sanny, J. and Moebs, W. (2021) Física Universitaria, Volumen 1. Openstax. https://openstax.org/details/books/física-universitaria-volumen-1

[12] Sherbon Hills, E. (1977) Elementos de geología estructural. Editorial Ariel.

[13] Gutiérrez, A.A. and Mon, R. (2008) Macroindicadores cinemáticos en el Bloque Ambato, provincias de Tucumán y Catamarca. *Revista de la Asociación Geológica Argentina*, **63**, 24-28.

[14] Gutierrez, A.A., Mon, R., Arnous, A. and Cisterna, C.E. (2019) Sinestral Rotation and NNW Shortening of the Ambato Block Induced by Cenozoic NE to E-W Transpression, Argentina. *International Journal of Earth Science and Geology*, **1**, 74-85. https://doi.org/10.18689/ijeg-1000109

[15] Naylor, M.A., Mandl, G. and Supesteijn, C.H.K. (1986) Fault Geometries in Basement-Induced Wrench Faulting under Different Initial Stress States. *Journal of Structural Geology*, **8**, 737-752. https://doi.org/10.1016/0191-8141(86)90022-2

[16] Woodcock, N.H. and Fischer, M. (1986) Strike-Slip Duplexes. *Journal of Structural Geology*, **8**, 725-735. https://doi.org/10.1016/0191-8141(86)90021-0

[17] Gutiérrez, A.A. (1999) Tectonic Geomorphology of the Ambato Block (Northwestern Pampeanas Mountain Ranges, Argentina). Fourth ISAG, Göettingen, 307-310.

[18] Gutiérrez, A.A., Mon, R., Cisterna, C.E., Altenberger, U. and Arnous, A. (2023) Cenozoic Age Counterclockwise Rotation in the Northwest End of the Sierras Pampeanas, Argentina. *Open Journal of Geology*, **13**, 345-383. https://doi.org/10.4236/ojg.2023.135018

[19] Milani, E.J. and Thomaz Filho, A. (2000) Sedimentary Basins of South America. 2000 31*st International Geological Congress*, Rio de Janeiro, 5-17 August 2000, 389-449.

[20] Iglesia Llanos, M.P. (2008) Paleogeografía de América del Sur durante el Jurásico. *Revista de la Asociación Geológica Argentina*, **63**, 498-511.

[21] Ramos, V.A. and Aleman, A. (2000) Tectonic Evolution of the Andes. In: Cordani,

U.G., Milani, E.J., Thomz Filo, A. and Campos, D.A., Eds., *Tectonic Evolution of South America*, 31° International Geological Congress, 635-685.

[22] Scotese, C.R. (1991) Jurassic and Cretaceous Plate Tectonic Reconstructions. *Palaeogeography, Palaeoclimatology, Palaeoecology*, **87**, 493-501. https://doi.org/10.1016/0031-0182(91)90145-h

[23] Lovecchio, J.P., Rohais, S., Ramos, V.A. and Bolatti, N. (2022) Rifting Mesozoico en el sudoeste de Gondwuana: influencia del rifting precedente en la apertura del océano Atlántico sur austral. 11*th Congreso de Exploración y Desarrollo de Hidrocarburos. Simposio sobre la Exploración Offshore en el Sector Sur del Margen Atlántico Sudamericano*, Mendoza, 8-11 November 2022, 15-44.

[24] Stewart, K., Turner, S., Kelley, S., Hawkesworth, C., Kirstein, L. and Mantovani, M. (1996) 3-D, 40ar 39ar Geochronology in the Paraná Continental Flood Basalt Province. *Earth and Planetary Science Letters*, **143**, 95-109. https://doi.org/10.1016/0012-821x(96)00132-x

[25] Franzese, J., Spalletti, L., Pérez, I.G. and Macdonald, D. (2003) Tectonic and Paleoenvironmental Evolution of Mesozoic Sedimentary Basins along the Andean Foothills of Argentina (32° - 54° S). *Journal of South American Earth Sciences*, **16**, 81-90. https://doi.org/10.1016/s0895-9811(03)00020-8

[26] https://www.stratigraphy.org

[27] Somoza, R., Vizán, H. and Taylor, G.K. (2008) Tectonic Rotations in the Deseado Massif, Southern Patagonia, during the Breakup of Western Gondwana. *Tectonophysics*, **460**, 178-185. https://doi.org/10.1016/j.tecto.2008.08.004

[28] Scotese, C.R., Gahagan, L.M. and Larson, R.L. (1988) Plate Tectonic Reconstructions of the Cretaceous and Cenozoic Ocean Basins. *Tectonophysics*, **155**, 27-48. https://doi.org/10.1016/0040-1951(88)90259-4

[29] Martino, R.D., Guereschi, A.B., Carignano, C.A., Calegari, R. and Manoni, R. (2014) La estructura de las cuencas extensionales cretácicas de las Sierras de Córdoba. *Relatorio del XIX Congreso Gelógico Argentino*, Córdoba, 2-6 June 2014, 513-538.

[30] Jaillard, E., Hérail, G., Monfret, T., Díaz-Martínez, E., Baby, P., Lavenu, A. and Dumont, J.F. (2000) Tectonic Evolution of the Andes of Ecuador, Perú, Bolivia and Northernmost Chile. In: Cordani, U.G., Milani, E.J., Thomaz Filho, A. and Campos, D.A., Eds., *Tectonic Evolution of South America*, 31° International Geological Congress, 481-559.

[31] Somoza, R. and Zaffarana, C.B. (2008) Mid-Cretaceous Polar Standstill of South America, Motion of the Atlantic Hotspots and the Birth of the Andean Cordillera. *Earth and Planetary Science Letters*, **271**, 267-277. https://doi.org/10.1016/j.epsl.2008.04.004

[32] Starck, D. (2011) Cuenca Cretácica-Paleógena del noroeste argentino. 8*th Congreso de Exploración y Desarrollo de Hidrocarburos Simposio Cuencas Argentinas: Visión Actua*l, Mar del Plata, 8-12 November 2011, 407-453.

[33] Galliski, M.A. and Viramonte, J.G. (1988) The Cretaceous Paleorift in Northwestern Argentina: A Petrologic Approach. *Journal of South American Earth Sciences*, **1**, 329-342. https://doi.org/10.1016/0895-9811(88)90021-1

[34] Costa, J.B.S., Léa Bemerguy, R., Hasui, Y. and da Silva Borges, M. (2001) Tectonics and Paleogeography along the Amazon River. *Journal of South American Earth Sciences*, **14**, 335-347. https://doi.org/10.1016/s0895-9811(01)00025-6

[35] Figueiredo, J., Hoorn, C., van der Ven, P. and Soares, E. (2009) Late Miocene Onset of the Amazon River and the Amazon Deep-Sea Fan: Evidence from the Foz Do

Amazonas Basin. *Geology*, **37**, 619-622. https://doi.org/10.1130/g25567a.1

[36] Barazangi, M. and Isacks, B.L. (1976) Spatial Distribution of Earthquakes and Subduction of the Nazca Plate beneath South America. *Geology*, **4**, 686-692. https://doi.org/10.1130/0091-7613(1976)4<686:sdoeas>2.0.co;2

[37] Barazangi, M. and Isacks, B.L. (1979) Subduction of the Nazca Plate beneath Peru: Evidence from Spatial Distribution of Earthquakes. *Geophysical Journal International*, **57**, 537-555. https://doi.org/10.1111/j.1365-246x.1979.tb06778.x

[38] Jordan, T.E., Isacks, B.L., Allmendinger, R.W., Brewer, J.A., Ramos, V.A. and Ando, C.J. (1983) Andean Tectonics Related to Geometry of Subducted Nazca Plate. *Geological Society of America Bulletin*, **94**, 341-361. https://doi.org/10.1130/0016-7606(1983)94<341:atrtgo>2.0.co;2

[39] Yañez, G. and Ranero, C. (1999) The Role of the Juan Fernandez Ridge in the Long Lived Andean Segmentation at 33.5° S. 4*th ISAG Göettingen*, Universitât Gôttingen, 4-6 October 1999, 815-819.

[40] Wagner, L.S., Beck, S. and Zandt, G. (2005) Upper Mantle Structure in the South Central Chilean Subduction Zone (30° to 36° S). *Journal of Geophysical Research*: *Solid Earth*, **110**, B01308. https://doi.org/10.1029/2004jb003238

[41] Somoza, R. (2008) Major Mid-Cretaceous Plate Reorganization as the Trigger of the Andean Orogeny. 7*th International Symposium on Andean Geodynamics*, Paris, 2-4 September 2008, 509-512.

[42] Trumbull, R.B., Riller, U., Oncken, O., Scheuber, E., Munier, K. and Hongn, F. (2006) The Time-Space Distribution of Cenozoic Volcanism in the South-Central Andes: A New Data Compilation and Some Tectonic Implications. In: *Frontiers in Earth Sciences*, Springer, 29-43. https://doi.org/10.1007/978-3-540-48684-8_2

[43] Bosio, P.P., Powell, J., Papa, C.d. and Hongn, F. (2009) Middle Eocene Deformation–Sedimentation in the Luracatao Valley: Tracking the Beginning of the Foreland Basin of Northwestern Argentina. *Journal of South American Earth Sciences*, **28**, 142-154. https://doi.org/10.1016/j.jsames.2009.06.002

[44] Carey, S.W. (1955) The Orocline Concept in Geotectonic. *Proceedings of the Royal Society of Tasmania*, **89**, 255-288.

[45] Isacks, B. (1988) Uplift of the Central Andean Plateau and Bending of the Bolivian Orocline. *Journal of Geophysical Research*, **93**, 3211-3231. https://doi.org/10.1029/JB093iB04p03211

[46] Assumpcao, M. (1992) The Regional Intraplate Stress Field in South America. *Journal of Geophysical Research*: *Solid Earth*, **97**, 11889-11903. https://doi.org/10.1029/91jb01590

[47] Allmendinger, R.W., González, G., Yu, J., Hoke, G. and Isacks, B. (2005) Trench-parallel Shortening in the Northern Chilean Forearc: Tectonic and Climatic Implications. *Geological Society of America Bulletin*, **117**, 89-104. https://doi.org/10.1130/b25505.1

[48] Ghidella, M.E., Lawver, L.A., Marenssi, S. and Gahagan, L.M. (2007) Modelos de cinemática de placas para Antártida durante la ruptura de Gondwuana: Una revisión. *Revista de la Asociación Geológica Argentina*, **62**, 635-645.

[49] Arriagada, C., Roperch, P., Mpodozis, C. and Cobbold, P.R. (2008) Paleogene Building of the Bolivian Orocline: Tectonic Restoration of the Central Andes in 2-D Map View. *Tectonics*, **27**, TC6014. https://doi.org/10.1029/2008tc002269

[50] Martinod, J., Husson, L., Roperch, P., Guillaume, B. and Espurt, N. (2010) Horizontal Subduction Zones, Convergence Velocity and the Building of the Andes. *Earth and*

Planetary Science Letters, **299**, 299-309. https://doi.org/10.1016/j.epsl.2010.09.010

[51] Gutiérrez, A.A. and Mon, R. (2017) La faja plegada de antepaís del norte de Argentina. 20*th Congreso Geológico Argentino*, Tucumán, 7-11 August 2017, 124-131.

[52] Arne, H.R., Kukowski, N., Dresen, G., Echtler, H., Oncken, O., Klotz, J., Scheuber, E. and Kellner, A. (2006) Oblique Convergence along the Chilean Margin: Partitioning, Margin-Parallel Faulting and Force Interaction at the Plate Interface. In: *The Andes*, *Active Subduction Orogeny*, Springer, 125-146.

[53] Torres Carbonell, P.J., Olivero, E.B. and Dimieri, L.V. (2008) Structure and Evolution of the Fuegian Andes Foreland Thrust-Fold Belt, Tierra Del Fuego, Argentina: Paleogeographic Implications. *Journal of South American Earth Sciences*, **25**, 417-439. https://doi.org/10.1016/j.jsames.2007.12.002

[54] Beck, M.E. (1988) Analysis of Late Jurassic-Recent Paleomagnetic Data from Active Plate Margins of South America. *Journal of South American Earth Sciences*, **1**, 39-52. https://doi.org/10.1016/0895-9811(88)90014-4

[55] Hartley, A.J., Jolley, E.J. and Turner, P. (1992) Paleomagnetic Evidence for Rotation in the Precordillera of Northern Chile: Structural Constraints and Implications for the Evolution of the Andean Forearc. *Tectonophysics*, **205**, 49-64. https://doi.org/10.1016/0040-1951(92)90417-5

[56] Beck, M.E., Burmester, R.R., Drake, R.E. and Riley, P.D. (1994) A Tale of Two Continents: Some Tectonic Contrasts between the Central Andes and the North American Cordillera, as Illustrated by Their Paleomagnetic Signatures. *Tectonics*, **13**, 215-224. https://doi.org/10.1029/93tc02398

[57] Randall, D.E., Taylor, G.K. and Grocott, J. (1996) Major Crustal Rotations in the Andean Margin: Paleomagnetic Results from the Coastal Cordillera of Northern Chile. *Journal of Geophysical Research*: *Solid Earth*, **101**, 15783-15798. https://doi.org/10.1029/96jb00817

[58] Arriagada, C., Ferrando, R., Córdova, L., Morata, D. and Roperch, P. (2013) El Oroclino del Maipo: Un rasgo estructural de primer orden en la evolución geodinámica Mioceno a Reciente en los Andes de Chile Central. *Andean Geology*, **40**, 419-437. https://doi.org/10.5027/andgeov40n3-a02

[59] Allmendinger, R.W., Ramos, V.A., Jordan, T.E., Palma, M. and Isacks, B.L. (1983) Paleogeography and Andean Structural Geometry, Northwest Argentina. *Tectonics*, **2**, 1-16. https://doi.org/10.1029/tc002i001p00001

[60] Cooper, M.A. and Addison, F.T. (1995) Basin Development and Tectonic History of the Llanos Basin, Eastern Cordillera, and Middle Magdalena Valley, Colombia. *AAPG Bulletin*, **79**, 1421-1443. https://doi.org/10.1306/7834d9f4-1721-11d7-8645000102c1865d

[61] Arriagada, C., Roperch, P. and Mpodozis, C. (2000) Clockwise Block Rotations along the Eastern Border of the Cordillera De Domeyko, Northern Chile (22˚45' - 23˚30' S). *Tectonophysics*, **326**, 153-171. https://doi.org/10.1016/s0040-1951(00)00151-7

[62] Arriagada, C., Roperch, P., Mpodozis, C., Dupont-Nivet, G., Cobbold, P.R., Chauvin, A., *et al.* (2003) Paleogene Clockwise Tectonic Rotations in the Forearc of Central Andes, Antofagasta Region, Northern Chile. *Journal of Geophysical Research*: *Solid Earth*, **108**, 10-22. https://doi.org/10.1029/2001jb001598

[63] McQuarrie, N. (2002) Initial Plate Geometry, Shortening Variations, and Evolution of the Bolivian Orocline. *Geology*, **30**, 867-870. https://doi.org/10.1130/0091-7613(2002)030<0867:ipgsva>2.0.co;2

[64] Ries, A.C. and Shackleton, R.M. (1976) Patterns of Strain Variation in Arcuate Fold

Belts. *Philosophical Transactions of the Royal Society of London*, **283**, 281-288.

[65] Johnston, S.T., Weil, A.B. and Gutierrez-Alonso, G. (2013) Oroclines: Thick and Thin. *Geological Society of America Bulletin*, **125**, 643-663. https://doi.org/10.1130/b30765.1

[66] Roperch, P., Sempere, T., Macedo, O., Arriagada, C., Fornari, M., Tapia, C., *et al.* (2006) Counterclockwise Rotation of Late Eocene-Oligocene Fore-Arc Deposits in Southern Peru and Its Significance for Oroclinal Bending in the Central Andes. *Tectonics*, **25**, TC3010. https://doi.org/10.1029/2005tc001882

[67] Mitouard, P., Kissel, C. and Laj, C. (1990) Post-Oligocene Rotations in Southern Ecuador and Northern Peru and the Formation of the Huancabamba Deflection in the Andean Cordillera. *Earth and Planetary Science Letters*, **98**, 329-339. https://doi.org/10.1016/0012-821x(90)90035-v

[68] Laj, C., Mitouard, P., Roperch, P., Kissel, C., Mourier, T. and Megard, F. (1989) Paleomagnetic Rotations in the Coastal Areas of Ecuador and Northern Peru. In: *Paleomagnetic Rotations and Continental Deformation*, Springer, 489-511. https://doi.org/10.1007/978-94-009-0869-7_29

[69] Kono, M., Heki, K. and Hamano, Y. (1985) Paleomagnetic Study of the Central Andes: Counterclockwise Rotation of the Peruvian Block. *Journal of Geodynamics*, **2**, 193-209. https://doi.org/10.1016/0264-3707(85)90010-9

[70] Tibaldi, A., Corazzato, C. and Rovida, A. (2009) Miocene–Quaternary Structural Evolution of the Uyuni–Atacama Region, Andes of Chile and Bolivia. *Tectonophysics*, **471**, 114-135. https://doi.org/10.1016/j.tecto.2008.09.011

[71] Egbue, O. and Kellogg, J. (2010) Pleistocene to Present North Andean "Escape". *Tectonophysics*, **489**, 248-257. https://doi.org/10.1016/j.tecto.2010.04.021

[72] Montes, C., Guzman, G., Bayona, G., Cardona, A., Valencia, V. and Jaramillo, C. (2010) Clockwise Rotation of the Santa Marta Massif and Simultaneous Paleogene to Neogene Deformation of the Plato-San Jorge and Cesar-Ranchería Basins. *Journal of South American Earth Sciences*, **29**, 832-848. https://doi.org/10.1016/j.jsames.2009.07.010

[73] Sager, W.W., Thoram, S., Engfer, D.W., Koppers, A.A.P. and Class, C. (2021) Late Cretaceous Ridge Reorganization, Microplate Formation, and the Evolution of the Rio Grande Rise—Walvis Ridge Hot Spot Twins, South Atlantic Ocean. *Geochemistry, Geophysics, Geosystems*, **22**, e2020GC009390. https://doi.org/10.1029/2020gc009390